medRxiv preprint doi: https://doi.org/10.1101/2024.07.11.24310281; this version posted December 7, 2024. The copyright holder for this preprint (which was not certified by peer review) is the author/funder, who has granted medRxiv a license to display the preprint in perpetuity. It is made available under a CC-BY 4.0 International license .

A Longitudinal and Reproducible Anti-coactivation Pattern Between the Cerebellum and the Ventral Tegmental Area Relates to Apathy in Schizophrenia

Authors

Farnaz Delavari[1,2]*, Jade Awada[3]*, Thomas A. W. Bolton[3], Fares Alouf[3], Fabien Carruzzo[6], Noemie Kuenzi[6], Mariia Kaliuzhna[6], Tal Geffen[7], Teresa Katthagen[7], Florian Schlagenhauf[7], Dimitri Van De Ville[4,5], Stephan Eliez[1], Stefan Kaiser[6,8], Indrit Bègue[3,8]

Affiliations

1. Developmental Imaging and Psychopathology Laboratory, University of Geneva School of Medicine, Geneva, Switzerland
2. Neuro-X Institute, École Polytechnique Fédérale de Lausanne, Switzerland
3. Neuroimaging and translational psychiatry lab, Department of psychiatry, University of Geneva, Switzerland
4. Institute of Bioengineering, Ecole Polytechnique de Fédérale de Lausanne (EPFL), Lausanne, Switzerland
5. Department of radiology and medical informatics, University of Geneva, Switzerland
6. Laboratory for experimental psychopathology, Department of psychiatry, University of Geneva, Switzerland

NOTE: This preprint reports new research that has not been certified by peer review and should not be used to guide clinical practice.

medRxiv preprint doi: https://doi.org/10.1101/2024.07.11.24310281; this version posted December 7, 2024. The copyright holder for this preprint (which was not certified by peer review) is the author/funder, who has granted medRxiv a license to display the preprint in perpetuity. It is made available under a CC-BY 4.0 International license .

7. Department of Psychiatry and Neurosciences, Campus Charité Mitte, Berlin, Germany
8. Adult psychiatry division, Department of psychiatry, University Hospitals of Geneva, Switzerland

*Shared authorship

Corresponding author

Indrit Bègue, indrit.begue@unige.ch

Laboratory for neuroimaging and translational psychiatry,

Department of psychiatry, University of Geneva, Switzerland

Campus Biotech, Chemin des Mines 9, 1202, Geneva Switzerland

Figures: 4

Tables: 2

medRxiv preprint doi: https://doi.org/10.1101/2024.07.11.24310281; this version posted December 7, 2024. The copyright holder for this preprint (which was not certified by peer review) is the author/funder, who has granted medRxiv a license to display the preprint in perpetuity. It is made available under a CC-BY 4.0 International license .

ABSTRACT

Background

Negative symptoms of schizophrenia lack effective treatments. Anomalies in the reward system and cerebellum have been linked to negative symptom The cerebellum modulates reward circuitry via the ventral tegmental area (VTA). The "cognitive dysmetria theory" posits that reduced cerebellar inhibition in schizophrenia may underlie striatal hyperdopaminergia. However, cerebellum-VTA connectivity and its impact on negative symptoms in schizophrenia remains unclear.

Methods

From 427 individuals screened, 146 participants were recruited: 90 with schizophrenia (SZ) and 56 healthy controls (HC). At 3 months (T2), 65 individuals (36 SZ, 29 HC) completed follow-up. SZ participants were invited for clinical interviews at 9 months (T3; 33 SZ). After quality check, 105 participants were retained at T1, 41 at T2, and 21 at T3. The validation cohort consisted of 53 individuals (28 SZ, 25 HC). The Brief Negative Symptom Scale was used to quantify negative symptoms. Dynamic functional connectivity of the cerebellum and VTA was analyzed using state-of-the-art coactivation patterns analysis.

Results

A reproducible cerebellum-VTA anti-coactivation pattern was found across T1 and T2 ($r = 0.98$) in bilateral paravermal Crus I/II. Lower anti-coactivation emergence at T1 correlated with worse apathy, particularly asociality and avolition. At T2, lower anti-coactivation persistence related to worse apathy, especially anhedonia, and correlated with worse anhedonia at T3. Similarly, reduced anti-coactivation emergence at T2 linked to worse asociality at T3. In the validation cohort, we replicated the anti-coactivation pattern ($r = 0.93$) and the correlation of its emergence with apathy, in particular, asociality.

medRxiv preprint doi: https://doi.org/10.1101/2024.07.11.24310281; this version posted December 7, 2024. The copyright holder for this preprint (which was not certified by peer review) is the author/funder, who has granted medRxiv a license to display the preprint in perpetuity. It is made available under a CC-BY 4.0 International license .

Conclusion: Reduced cerebellum-VTA anti-coactivation is a reproducible neural marker of apathy in schizophrenia, highlighting its potential as a target for therapeutic intervention.

medRxiv preprint doi: https://doi.org/10.1101/2024.07.11.24310281; this version posted December 7, 2024. The copyright holder for this preprint (which was not certified by peer review) is the author/funder, who has granted medRxiv a license to display the preprint in perpetuity. It is made available under a CC-BY 4.0 International license .

INTRODUCTION

Negative symptoms in schizophrenia – a chronic psychiatric condition affecting up to 1% of the population – are marked by features such as apathy (asociality, anhedonia and avolition) or diminished expression (blunted affect, alogia) (1). Negative symptoms represent a key unmet need in psychiatry due to their profound effect on social functioning, their prevalence across various stages of the disorder and antipsychotic medication resistance (1). Therefore, a better understanding of the underlying mechanisms and pathways involved in negative symptoms in schizophrenia is crucial for advancing treatment options.

Recent conceptualizations of negative symptoms have evolved to map these symptoms onto two dimensions: apathy, manifesting as reductions in goal-directed behavior (avolition), pleasure (anhedonia) and social communication (asociality), and diminished expression in the emotional and verbal domains (blunted affect and alogia, respectively) (2). Emerging evidence highlights a link between negative symptoms, in particular apathy, and dysfunctions in the reward system including the Ventral Tegmental Area (VTA; mesolimbic pathway) (3,4). Parallel to these findings, the cerebellum, traditionally recognized for its role in motor coordination, has been increasingly implicated in reward processing (5), social and emotional learning (6), and the pathophysiology of negative symptoms in schizophrenia (4,7). From early neuroimaging to modern day research, cerebellar vermis structural reduction (8) and altered cerebellar-cortical functional connectivity (9–11) have pointed to a key role of the cerebellum in schizophrenia.

medRxiv preprint doi: https://doi.org/10.1101/2024.07.11.24310281; this version posted December 7, 2024. The copyright holder for this preprint (which was not certified by peer review) is the author/funder, who has granted medRxiv a license to display the preprint in perpetuity. It is made available under a CC-BY 4.0 International license .

A seminal theory on cerebellar involvement in schizophrenia was conceptualized with the Cognitive Dysmetria Theory (12), given links between forebrain hyperdopaminergia and cerebellar vermis malfunction from reductions in Purkinje cell size and density in post-mortem studies (13). This theory postulated that malfunction of the cerebellar cortex would lead to disinhibition of excitatory projections from the deep nuclei to dopaminergic neurons in the midbrain, resulting in a "hyperdopaminergic state" (14). Consistent with this hypothesis, Daskalakis et al. (2005) examined cerebellar brain inhibition in patients with schizophrenia and found an almost 30% reduction compared to healthy controls (15). Cerebellar brain inhibition refers to the inhibitory tone exerted by the cerebellum on motor neural circuits manifested as a reduction in motor evoked potential when the cerebellum is stimulated 5-7 ms prior to the motor cortex (16). These findings raise the possibility that the cerebellum may be implicated in the negative symptoms pathophysiology via the exertion of modulatory role on the reward system (17), analogous to its established role on motor control. This hypothesis is grounded in several mechanistic insights tying the cerebellum to reward circuitry: 1) activity within the cerebellum during reward anticipation has been consistently observed in human neuroimaging (18) and rodent studies (19); 2) direct monosynaptic connections from the deep cerebellar nuclei to the VTA have been documented in both animal (20–22) and human studies (23–25); 3) the cerebellum exerts an inhibitory tone on the circuit of Papez (24) and its stimulation was found to be associated to ‘pleasure’ and stopping of seizure starting from the hippocampus (25). In addition, the cerebellum's contribution to the negative symptoms pathophysiology, especially through its effects on the reward system, can be understood by considering its intrinsic role in coordinating and timing of neural processes (5). Thus, in sum, the cerebellum's

medRxiv preprint doi: https://doi.org/10.1101/2024.07.11.24310281; this version posted December 7, 2024. The copyright holder for this preprint (which was not certified by peer review) is the author/funder, who has granted medRxiv a license to display the preprint in perpetuity. It is made available under a CC-BY 4.0 International license .

capacity to integrate inputs relevant to reward processing and modulate reward-related activities through precise timing and coordination, could underlie the mechanisms behind cerebellar contributions to the negative symptom pathophysiology.

A key role for the cerebellum with high therapeutic potential to address negative symptoms is further supported from recent non-invasive cerebellar neuromodulation evidence, convergently indicating improvement in negative symptoms severity (26). Active (but not sham) cerebellar transcranial magnetic stimulation (TMS) increased resting-state functional connectivity between the vermian and pallidal areas (27), suggesting a functional linkage with regions in the reward circuitry. Overall, this evidence suggests that the cerebellum's connectivity with the reward system, especially its interactions with the VTA, should provide clinically relevant insights. However, the functional connectivity between the cerebellum and the VTA in the context of negative symptoms remains largely unknown and has not been examined in schizophrenia.

In this research, we set out to investigate for the first time the connectivity between the cerebellum and the VTA across three time points [baseline (T1), at 3 months (T2) and 9 months (T3) after baseline] in a well-characterized cohort of patients with schizophrenia. To strengthen the generalizability of our findings, we employed an additional independently acquired validation cohort. We leveraged a well-established dynamic functional connectivity approach, coactivation pattern (CAP) analysis (28,29), to capture transient neural coactivation events between the cerebellum and VTA during resting-state. We focused on the VTA as the seed region and extracted

medRxiv preprint doi: https://doi.org/10.1101/2024.07.11.24310281; this version posted December 7, 2024. The copyright holder for this preprint (which was not certified by peer review) is the author/funder, who has granted medRxiv a license to display the preprint in perpetuity. It is made available under a CC-BY 4.0 International license .

its spatial patterns of coactivation within the cerebellum. We subsequently derived metrics related to these spatial patterns: emergence (*i.e.*, CAP entry frequency, quantifying the number of times a certain pattern of coactivation occurred from VTA below-threshold activity) and persistence (*i.e.*, CAP duration, quantifying the time in seconds a certain pattern of coactivation persisted upon occurring). We hypothesized that the features of the dynamic functional connectivity patterns between the VTA and the cerebellum during resting-state were linked to schizophrenia clinical manifestations and would represent a functional signature of negative symptoms in schizophrenia over time.

medRxiv preprint doi: https://doi.org/10.1101/2024.07.11.24310281; this version posted December 7, 2024. The copyright holder for this preprint (which was not certified by peer review) is the author/funder, who has granted medRxiv a license to display the preprint in perpetuity. It is made available under a CC-BY 4.0 International license .

METHODS

Data Collection

We systematically collected demographic, clinical, cognitive, behavioral, and neuroimaging data in a main cohort and a validation cohort.

For the main cohort, from 427 individuals screened, we recruited 146 individuals (90 patients with schizophrenia spectrum disorder (SZ) and 56 healthy controls (HC) at baseline, 65 individuals (36 SZ and 29 HC) at 3 months after baseline (T2), and 33 SZ at 9 months after baseline (T3) (refer to the screening process in Table S1 in the Supplemental Materials). Participants were administered a series of interviews and neuroimaging protocols at T1 and T2, and only interviews at T3. The cohort was recruited in the context of two studies approved by the Geneva Ethics Committee in Switzerland (CCER. BASEC ID: 2017-01765 and 2020-02169). The validation cohort was acquired in the context of the SyMoNe study ("Neural and behavioral markers for the motivational negative symptoms of schizophrenia – a longitudinal approach"; trial registration: DRKS00011405).

We recruited clinically stable patients with schizophrenia (*i.e.*, no changes in medication and no hospitalizations in the last 3 months). Patients had confirmed schizophrenia diagnosis via the Mini International Neuropsychiatric Interview (30). Given our focus in obtaining mechanistical insights and in accordance with recent recommendations (1), we excluded patients with secondary sources of negative symptoms (*e.g.*, psychosis, extrapyramidal effects, medication, depression, sedation;

medRxiv preprint doi: https://doi.org/10.1101/2024.07.11.24310281; this version posted December 7, 2024. The copyright holder for this preprint (which was not certified by peer review) is the author/funder, who has granted medRxiv a license to display the preprint in perpetuity. It is made available under a CC-BY 4.0 International license .

see exclusion criteria in Supplemental material). Patients were recruited from community outpatient centers in the University Hospital of Geneva, Switzerland for the main cohort and from outpatient clinics at the Department of Psychiatry and Psychotherapy of Charité – Universitätsmedizin Berlin for the validation cohort (see Figure S1 in Supplemental Materials).

Clinical psychopathological and cognitive assessment

In both cohorts, all individuals (HC and SZ) underwent a detailed psychopathological and cognitive assessment (see Supplemental Materials for comprehensive description of the assessment). To assess the negative symptoms in patients with schizophrenia, we used the Brief Negative Symptoms Scale (BNSS) (1), a semi-structured interview conducted by trained researchers/clinicians. The BNSS is a second-generation instrument based on the NIMH-MATRICS consensus statement that is now widely recommended (2).

Acquisition of neuroimaging data

MRI data for the main cohort were acquired at the Campus Biotech (Geneva, Switzerland) using a Siemens 3T Magnetom Prisma scanner and a standard 64 channel head coil and high-resolution resting-state images were captured with specified parameters (voxel size: 2.0 × 2.0 × 2.0 mm^3, repetition time = 1000 ms). Full details of acquisition parameters of neuroimaging scans are available in the Supplemental Materials. MRI data for the validation cohort were acquired with the same acquisition protocol.

medRxiv preprint doi: https://doi.org/10.1101/2024.07.11.24310281; this version posted December 7, 2024. The copyright holder for this preprint (which was not certified by peer review) is the author/funder, who has granted medRxiv a license to display the preprint in perpetuity. It is made available under a CC-BY 4.0 International license .

Images then underwent standard preprocessing involving the following steps: 1) quality assessment and realignment of functional images, 2) co-registration and segmentation using DARTEL, 3) spatial normalization to MNI space and smoothing with a 6 mm full with at half maximum Gaussian kernel, 4) exclusion of the first five scans for signal stabilization, 5) linear detrending and nuisance regression using DPARSF tissue masks (33), 6) motion correction through scrubbing of high-motion frames and 7) quality check (see Supplemental Materials for full details).

Extraction of VTA-cerebellum CAPs and their spatiotemporal properties

Neural activity during rest is organized into time-varying, recurrent patterns of cross-regional interactions that can be captured via dynamic resting-state functional connectivity approaches. In this study, we examined the dynamic connectivity between the cerebellum and VTA through coactivation pattern (CAP) analysis (28,29), an established approach that has already contributed to the study of various psychiatric disorders (34,35) and is implemented in the publicly available *TbCAPs* toolbox (36) (Figure S1 in Supplemental Materials). In brief, timepoints with pronounced VTA activity are identified. Then, cerebellar activity at the same timepoints is retained and clustered into a set of spatial patterns, one of which is expressed at each of the retained timepoints. These patterns indicate functionally relevant networks within the cerebellum during episodes of VTA activation.

We identified the VTA using the left and right VTA masks of the Automated Anatomical Labeling (AAL) atlas (37).

medRxiv preprint doi: https://doi.org/10.1101/2024.07.11.24310281; this version posted December 7, 2024. The copyright holder for this preprint (which was not certified by peer review) is the author/funder, who has granted medRxiv a license to display the preprint in perpetuity. It is made available under a CC-BY 4.0 International license .

For each rs-fMRI session, the BOLD signal time-series from voxels within the bilateral VTA were extracted, averaged, and standardized (Z-scored). We selected timepoints with an average value exceeding a defined threshold. Consistent with the literature, a threshold of 0.5 was employed to allow the inclusion of more timepoints and ensure robust clustering at T1, when the biggest cohort of participants was involved (38). For the smaller cohort at T2 and for the validation sample, we employed a more stringent threshold of 1 to focus only on the timepoints with largest VTA activity (36,39). Only timepoints with framewise displacement lower than 0.5 mm (scrubbing) were retained, in line with current recommendations (28).

Selected volumes underwent *K*-means clustering to extract cerebellar CAPs. Clustering was run separately on the main cohort at T1, and on the validation cohort. In both cases, the optimal number of clusters was inferred from a train-and-test approach, resulting in four CAPs in the main cohort and seven CAPs in the validation cohort (see Supplemental Materials for details). Clustering was then also run on the main cohort at T2 for four CAPs.

To quantify the longitudinal stability of CAPs, we calculated pairwise Pearson correlations between the maps obtained at T1 and at T2. Scatterplots of the correlations are provided for each group and cohort in the Supplemental Materials (Figures S4 and S5).

All CAPs were visualized using cerebellar flatmaps (40). Voxel-wise signal values were converted to t-values, using the formula:

medRxiv preprint doi: https://doi.org/10.1101/2024.07.11.24310281; this version posted December 7, 2024. The copyright holder for this preprint (which was not certified by peer review) is the author/funder, who has granted medRxiv a license to display the preprint in perpetuity. It is made available under a CC-BY 4.0 International license .

$$t = \frac{x}{\frac{s}{\sqrt{n}}}$$

where x is the average BOLD value for the voxel at hand across the frames in which the CAP of interest is expressed, s is the standard deviation, and n is the number of frames. These maps effectively quantify the extent and stability of voxel activity within each dynamic state.

Two complementary metrics reflective of CAP temporal dynamics were calculated as described in (36) (Figure S1): *persistence*, or the average time, in seconds, a CAP was consecutively expressed upon occurrence, and *emergence*, denoting the frequency, irrespective of duration, at which a specific CAP occurred after VTA under-threshold activity.

Exploration of the relation of CAP metrics with negative symptoms

Statistical analyses included non-parametric testing with rank tests for median comparisons to contrast CAP metrics across groups, and Spearman's correlation to examine the associations of these metrics with psychopathology. Non-parametric testing allows for analyses without assumptions about data distribution. To evaluate the statistical significance of partial correlations given the relatively small sample size, non-parametric permutation testing with 5000 iterations was also employed (see Supplemental Materials for more details). These analyses were conducted in Python 3.9 using *statsmodels* (version 0.14.1). Throughout this work, the False Discovery Rate (FDR) was controlled using the Benjamini-Hochberg procedure to

medRxiv preprint doi: https://doi.org/10.1101/2024.07.11.24310281; this version posted December 7, 2024. The copyright holder for this preprint (which was not certified by peer review) is the author/funder, who has granted medRxiv a license to display the preprint in perpetuity. It is made available under a CC-BY 4.0 International license .

adjust p-values for multiple comparisons. All significant results survive FDR correction at a significant level of $p<0.05$ unless reported otherwise. To account for movement in the scanner and medication intake, unless specified otherwise, framewise displacement and risperidone equivalent dose were included as covariates in group comparisons of CAP metrics and partial correlation analyses with psychopathology through ANCOVA as implemented in Python 3.9 using the *statsmodels* and *pingouin* libraries (version 0.14.1).

For the main cohort at T1, the HC and SZ groups were contrasted, for each CAP, in terms of emergence and persistence. CAPs for which a significant group difference was found were further examined in terms of associations of the metrics with the severity of negative symptoms (apathy and diminished expression) as measured by the BNSS. A similar process was then performed at T2, and on the validation dataset, on the CAPs matching those of interest brought about at T1. Note that in the validation dataset, we examined the specific hypothesis derived from the main cohort through one-tailed tests.

The code for the above analyses can be found at: https://drive.google.com/drive/folders/1roAKf33fQ1S_q0uajCnlcPQvlV8-Th6t?usp=drive_link. All figures in this manuscript are generated in Biorender (https://BioRender.com).

medRxiv preprint doi: https://doi.org/10.1101/2024.07.11.24310281; this version posted December 7, 2024. The copyright holder for this preprint (which was not certified by peer review) is the author/funder, who has granted medRxiv a license to display the preprint in perpetuity. It is made available under a CC-BY 4.0 International license .

RESULTS

Demographic, neuroimaging, and clinical data in the main cohort

A summary of the main cohort characteristics from T1 to T3 can be found in Table 1. In this cohort, the patient population was matched for age and sex to healthy controls and included chronic and clinically stable patients with low levels of psychosis, depression and extrapyramidal syndrome. Negative symptoms in the patients' cohort were enduring from T1 to T3 and not associated with psychosis, medication, cognitive dysfunction, or extrapyramidal effects, suggesting that these symptoms were unconfounded by other clinical factors (see Supplemental Materials). This allows us to obtain a mechanistic understanding of the biological mechanisms driving negative symptoms.

Table 1. Demographic and psychopathology characteristics of study participants (main cohort)

Table 1. Demographic and psychopathology characteristics of study participants (main cohort)												
Demographics												
T1						T2					T3	
Group	SZ (N=58)		HC (N=47)			SZ (N=22)		HC (N=19)			SZ (N=21)	
	Mean	SD	Mean	SD	*p*	Mean	SD	Mean	SD	*p*	Mean	SD
Age	36.138	9.391	38.745	7.540	0.126 (two-sample t-test)	37.682	10.799	38.158	6.882	0.870 (two-sample t-test)	37.571	11.052
Sex (percentage of males)	84.5%		70.2%		0.128 (Chi-square test)	81.8%		84.2%		0.732 (Chi-square test)	80.9%	
Neuroimaging												
	Mean	SD	Mean	SD	*p*	Mean	SD	Mean	SD	*p*		
Mean framewise displacement during rs-fMRI	0.262	0.104	0.200	0.088	0.002 (two-sample t-test)	0.276	0.113	0.197	0.091	0.020 (two-sample t-test)	#	

Clinical and psychopathology information						
Group	SZ at T1 (N=58)		SZ at T2 (N=22)		SZ at T3 (N=21)	
Negative symptoms	Mean	SD	Mean	SD	Mean	SD
BNSS diminished expression	6.655	7.097	7.000	7.051	6.238	5.761
BNSS apathy	12.466	8.672	11.409	9.231	11.095	8.927

medRxiv preprint doi: https://doi.org/10.1101/2024.07.11.24310281; this version posted December 7, 2024. The copyright holder for this preprint (which was not certified by peer review) is the author/funder, who has granted medRxiv a license to display the preprint in perpetuity. It is made available under a CC-BY 4.0 International license .

Psychosis						
PANSS psychosis	9.603	2.655	9.182	2.612	9.762	3.192
Depression						
CDS	2.190	3.080	2.318	3.168	1.666	2.415
Cognition						
BACS	35.672	10.743	33.955	13.185	37.762	11.287
Psychosocial functioning						
PSP	4.397	1.736	5.091	1.444	5.095	1.758
Antipsychotic medication						
Dose in risperidone equivalent	4.509	2.629	4.420	2.407	4.652	2.814
Extrapyramidal syndrome						
SHRS	1.017	0.827	1.136	1.246	1.143	1.195
Number of hospitalizations in last 6 months*	0.075	0.267	#		#	
Duration of illness (years)**	12.038	7.488	#		#	

Abbreviations: SZ = schizophrenia; HC = healthy controls; SD = standard deviation; rs-fMRI = resting-state functional magnetic resonance imaging;

medRxiv preprint doi: https://doi.org/10.1101/2024.07.11.24310281; this version posted December 7, 2024. The copyright holder for this preprint (which was not certified by peer review) is the author/funder, who has granted medRxiv a license to display the preprint in perpetuity. It is made available under a CC-BY 4.0 International license .

BNSS = Brief Negative Symptom Scale; PANSS = Positive and Negative Syndrome Scale; CDS = Calgary Depression Scale for Schizophrenia; BACS = Brief Assessment of Cognition in Schizophrenia; PSP = Personal and Social Performance Scale; SHRS = St. Hans Rating Scale.

*Data not available for 2 patients.

**Data not available for 6 patients.

Data not available.

medRxiv preprint doi: https://doi.org/10.1101/2024.07.11.24310281; this version posted December 7, 2024. The copyright holder for this preprint (which was not certified by peer review) is the author/funder, who has granted medRxiv a license to display the preprint in perpetuity. It is made available under a CC-BY 4.0 International license .

medRxiv preprint doi: https://doi.org/10.1101/2024.07.11.24310281; this version posted December 7, 2024. The copyright holder for this preprint (which was not certified by peer review) is the author/funder, who has granted medRxiv a license to display the preprint in perpetuity. It is made available under a CC-BY 4.0 International license .

Investigation of cerebellar temporal coupling with the VTA at T1

Our neuroimaging analysis uncovered four spatially distinct cerebellum–VTA CAPs (Figure 1A; refer to the Supplemental Materials for the selection of the optimal number of clusters).

CAP1 was identified as a cerebellar anti-coactivation pattern with the VTA and was strongest at bilateral paravermal regions of Crus I and II. CAP2 showed coactivation with the VTA within lobule VI extending to Crus I and II. CAP3 encompassed mainly cerebellar signal in the anterior (lobules I-V) and posterior (lobules VIIIA and VIIIB) lobes. Finally, CAP4 showed anti-coactivation of the VTA predominantly with lateral Crus I and lobule VI.

medRxiv preprint doi: https://doi.org/10.1101/2024.07.11.24310281; this version posted December 7, 2024. The copyright holder for this preprint (which was not certified by peer review) is the author/funder, who has granted medRxiv a license to display the preprint in perpetuity. It is made available under a CC-BY 4.0 International license .

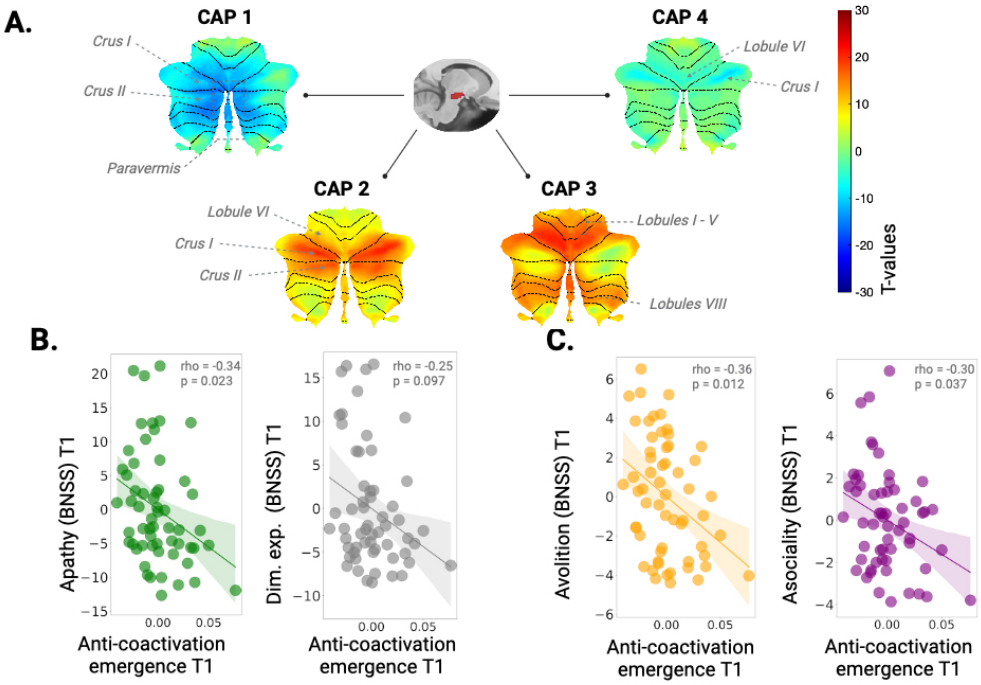

Figure 1. Spatial patterns of coactivation between the cerebellum and the VTA in patients (SZ) and controls (HC) and their relation to negative symptoms at T1. A. Distinct spatial maps of cerebellar coactivation with the VTA. B. Reduced anti-coactivation pattern emergence (CAP1 entry frequency) is associated with greater severity of apathy (in green) but not diminished expression (in grey). C. Reduced anti-coactivation pattern emergence (CAP1 entry frequency) is associated with greater severity of avolition (in yellow) and of asociality (in purple). *Note. Negative symptoms quantified by the Brief Negative Symptom Scale (BNSS). Greater scores indicate more severe symptoms. Dim. exp. = diminished expression. The colorbar represents T-values. Correlations are corrected for movement (mean framewise displacement) and antipsychotic medication (risperidone equivalent). Shaded areas on correlation plots B. and C. represent the 95% confidence interval.*

medRxiv preprint doi: https://doi.org/10.1101/2024.07.11.24310281; this version posted December 7, 2024. The copyright holder for this preprint (which was not certified by peer review) is the author/funder, who has granted medRxiv a license to display the preprint in perpetuity. It is made available under a CC-BY 4.0 International license .

At T1, CAP1 persistence is reduced in schizophrenia and its emergence relates to apathy but not diminished expression

We compared each CAP's persistence (average duration in seconds) and emergence (number of times a specific pattern emerges after VTA under-threshold activity) between patients with schizophrenia and HC and, found a significantly shorter CAP1 duration in patients ($F(1,103) = 16.13$, $p = 0.0009$, without covariates). Correction for antipsychotic dosage in patients (quantified by risperidone equivalents) and mean framewise displacement did not affect this result ($F(1,101) = 5.609$, $p = 0.02$). We found no significant differences in the persistence of the remaining three CAPs across the two diagnostic groups. Further, we found no significant differences in CAP emergence between the groups. Therefore, we focused on the clinical relevance of CAP1 for patients, by assessing the association between its temporal features (emergence and persistence) and negative symptoms (apathy and diminished expression as quantified by the BNSS subscales).

We found that CAP1 persistence was not associated with apathy or diminished expression. CAP1 emergence was significantly negatively correlated with the severity of apathy (*rho* = -0.31, $p = 0.035$; Figure 1B, left panel, without covariates), while the association with the severity of diminished expression was not significant (*rho* = -0.25, $p = 0.099$; Figure 1B, right panel, without covariates). Correction for antipsychotic dosage (quantified by risperidone equivalents) and mean framewise displacement yielded similar results (apathy: *rho* = -0.34, $p = 0.023$; diminished expression: *rho* = -0.25, $p = 0.097$).

medRxiv preprint doi: https://doi.org/10.1101/2024.07.11.24310281; this version posted December 7, 2024. The copyright holder for this preprint (which was not certified by peer review) is the author/funder, who has granted medRxiv a license to display the preprint in perpetuity. It is made available under a CC-BY 4.0 International license .

To gain a more detailed understanding of the relationship with apathy, we examined the individual apathy symptoms (i.e., avolition, asociality, and anhedonia) and observed that CAP1 emergence was associated with avolition (*rho* = -0.36, p = 0.012; Figure 1C, left panel) and asociality (*rho* = -0.3, p = 0.037; Figure 1C, right panel), but not with anhedonia (*rho* = -0.24, p = 0.102). Non-parametric permutation testing also confirmed these results (apathy: *rho* = -0.34, p = 0.012; avolition: *rho* = -0.36, p = 0.007; and asociality: *rho* = -0.30, p = 0.024) (see Figure S9 in the Supplemental Materials).

Investigation of cerebellar temporal coupling with the VTA at T2

Reproducible anti-coactivation pattern of the cerebellum with VTA in two distinct recordings

Like at T1, we identified four distinct cerebellum-VTA CAPs at T2 (Figure 2A). Comparison of spatial similarity at T1 and T2 using pairwise spatial correlation revealed an almost identical spatial equivalent of the cerebellar anti-coactivation (r = 0.98, $p < 0.001$) at T2, in favor of a reproducible functional signature (Figure 2B; see also Figures S4 and S5 in Supplemental Materials). For simplicity, we also refer to this almost identical pattern at T2 as CAP1 in what follows.

medRxiv preprint doi: https://doi.org/10.1101/2024.07.11.24310281; this version posted December 7, 2024. The copyright holder for this preprint (which was not certified by peer review) is the author/funder, who has granted medRxiv a license to display the preprint in perpetuity. It is made available under a CC-BY 4.0 International license .

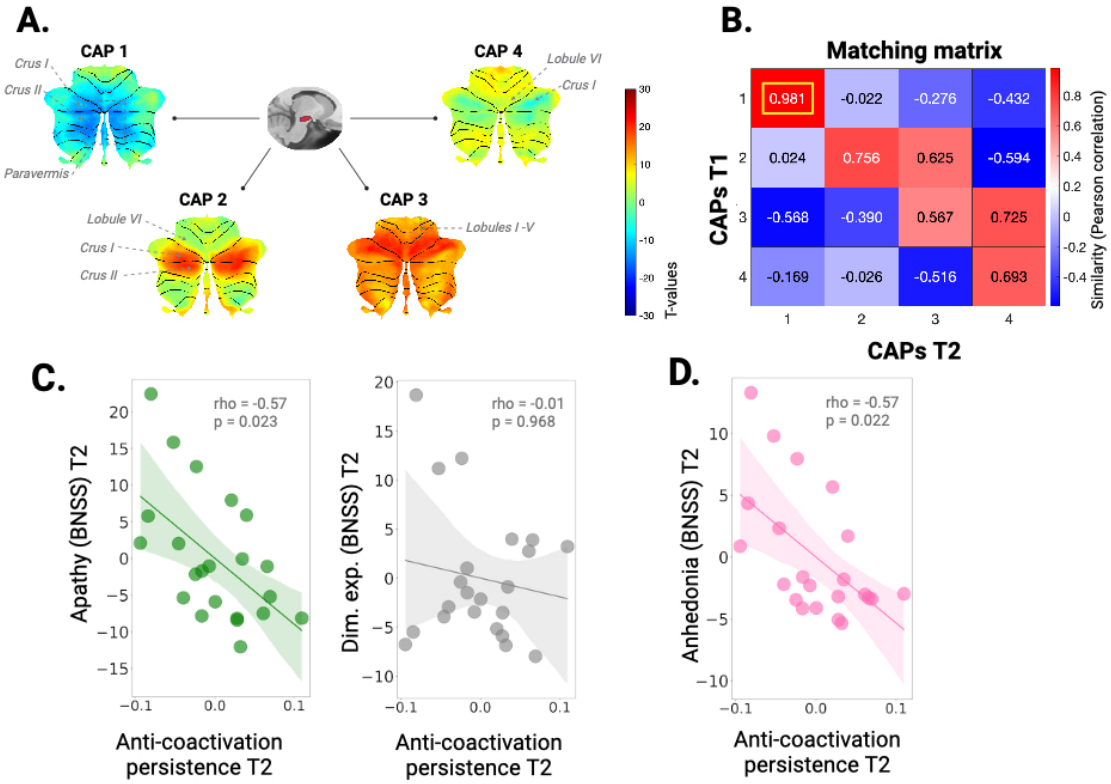

Figure 2. Spatial patterns of coactivation between the cerebellum and the VTA in patients (SZ) and controls (HC) and their relation to negative symptoms at T2. A. Distinct spatial maps of cerebellar coactivation with the VTA**.** B. Correlation matrix between patterns of coactivation at T1 and at T2. C. Reduced anti-coactivation persistence (CAP1 duration in seconds) is associated with greater severity of apathy (in green) but not diminished expression (in grey). D. Reduced anti-coactivation persistence is associated with greater severity of anhedonia (in pink). *Note. Negative symptoms are quantified by the Brief Negative Symptom Scale (BNSS). Greater scores indicate more severe symptoms. Dim. exp. = diminished expression. The colorbar in panel A represents T-values, while that in panel B depicts similarity (Pearson correlation). Correlations are corrected for movement (mean framewise displacement) and antipsychotic medication (risperidone equivalent). Shaded areas on correlation plots C. and D. represent the 95% confidence interval.*

medRxiv preprint doi: https://doi.org/10.1101/2024.07.11.24310281; this version posted December 7, 2024. The copyright holder for this preprint (which was not certified by peer review) is the author/funder, who has granted medRxiv a license to display the preprint in perpetuity. It is made available under a CC-BY 4.0 International license .

Anti-coactivation pattern persistence is reduced in schizophrenia and relates to apathy at T2

We examined the anti-coactivation pattern persistence and emergence between patients with schizophrenia and HC, and like at T1, found a significantly shorter duration in patients at T2 ($F(1,29) = 6.97$, $p = 0.026$). Persistence was also significantly negatively correlated with the severity of apathy (*rho* = -0.57, p = 0.023; Figure 2C, left panel) but not of diminished expression (*rho* = -0.01, p = 0.968; Figure 2C, right panel). By contrast, CAP1 emergence did not relate to negative symptom severity.

Again, we sought to obtain a more granular understanding of the relationship with apathy at T2, and examined the association with the individual items: anhedonia, asociality and avolition. We observed that CAP1 persistence was associated with anhedonia (*rho* = -0.57, p = 0.022), but neither with asociality nor with avolition (*rho* = -0.4, p = 0.167, *rho* = -0.3, p = 0.308, respectively). In sum, these findings suggest a distinct mapping of apathy subdomains to specific anti-coactivation metrics, with persistence putatively linked to anhedonia (as seen at T2) and emergence potentially associated with asociality or avolition (as observed at T1). We replicated the results using non-parametric permutations testing (apathy: *rho* = - 0.57, p = 0.008; anhedonia: *rho* = -0.57, p = 0.009) (see Figure S10 in the Supplemental Materials).

medRxiv preprint doi: https://doi.org/10.1101/2024.07.11.24310281; this version posted December 7, 2024. The copyright holder for this preprint (which was not certified by peer review) is the author/funder, who has granted medRxiv a license to display the preprint in perpetuity. It is made available under a CC-BY 4.0 International license .

Anti-coactivation pattern metrics at T2 are associated with apathy at T3

Finally, we asked whether CAP1 metrics at T1 or at T2 could be linked to symptoms at T3. We found that CAP1 metrics at T1 were not associated with apathy or diminished expression at T2 or T3. By contrast, the persistence of the anti-coactivation pattern at T2 correlated negatively with the severity of apathy at T3 (*rho* = -0.48, p = 0.049; Figure 3A, left panel), but not with that of diminished expression (*rho* = -0.2, p = 0.412; Figure 3A, right panel).

A more detailed examination uncovered that CAP1 *persistence* related to anhedonia (*rho* = -0.56, p = 0.035; Figure 3B, left panel) while CAP1 *emergence* related to asociality (*rho* = -0.55, p = 0.036; Figure 3B, right panel), replicating the previous findings of a differential relationship of anti-coactivation metrics with distinct negative symptoms observed at T1 and T2. Non-parametric permutations testing confirmed these results (apathy: *rho* = -0.48, p = 0.042; anhedonia: *rho* = -0.56, p = 0.014; asociality: *rho* = -0.55, p = 0.013)(see Figure S11 in the Supplemental Materials).

medRxiv preprint doi: https://doi.org/10.1101/2024.07.11.24310281; this version posted December 7, 2024. The copyright holder for this preprint (which was not certified by peer review) is the author/funder, who has granted medRxiv a license to display the preprint in perpetuity. It is made available under a CC-BY 4.0 International license .

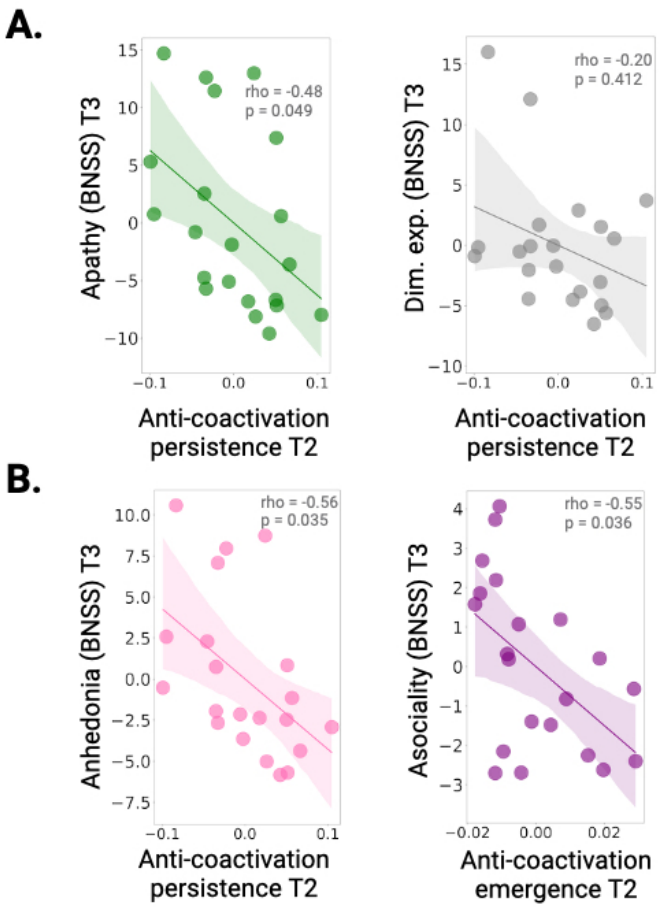

Figure 3. Relation between anti-coactivation metrics at T2 and negative symptoms at T3. A. Reduced anti-coactivation persistence (CAP1 duration in seconds) is associated with greater severity of apathy (in green) but not diminished expression (in grey). B. Reduced anti-coactivation persistence is associated with greater severity of anhedonia (in pink), while reduced anti-coactivation emergence (CAP1 entry frequency) is associated with greater severity of asociality (in purple). *Note. Negative symptoms are quantified by the Brief Negative Symptom Scale (BNSS). Greater scores indicate more severe symptoms. Dim. exp. = diminished expression. Correlations are corrected for movement (mean framewise displacement) and antipsychotic medication (risperidone equivalent). Shaded areas on correlation plots represent the 95% confidence interval.*

medRxiv preprint doi: https://doi.org/10.1101/2024.07.11.24310281; this version posted December 7, 2024. The copyright holder for this preprint (which was not certified by peer review) is the author/funder, who has granted medRxiv a license to display the preprint in perpetuity. It is made available under a CC-BY 4.0 International license .

Validation dataset analyses

A summary of the validation cohort characteristics across timepoints can be found in Table 2.

The validation cohort's population was matched for age and sex to healthy controls and included chronic and clinically stable patients with similar levels of negative symptoms to the main cohort (see Table S4 in Supplemental Materials). Both cohorts were also similar for other clinical parameters like medication, cognitive dysfunction, or extrapyramidal effects. However, patients in the validation cohort had relatively higher psychosis scores compared to patients in the main cohort (see Tables S4 and S5 in Supplemental Materials for uncorrected results).

Table 2. Demographic and psychopathology characteristics of study participants (validation cohort)

Table 2. Demographic and psychopathology characteristics of study participants (validation cohort)					
Demographics					
Group	SZ (N=28)		HC (N=25)		
	Mean	SD	Mean	SD	*p*
Age	37.4	7.280	38.571	9.979	0.625 (two-sample t-test)
Sex (percentage of males)	78.6%		76%		0.639 (Chi-square test)
Neuroimaging					
	Mean	SD	Mean	SD	*p*
Mean framewise displacement during rs-fMRI	0.310	0.083	0.248	0.070	0.005 (two-sample t-test)
Clinical and psychopathology information					
SZ (N=28)					
Negative symptoms	Mean		SD		
BNSS diminished expression	7.107		6.973		
BNSS apathy	15.036		9.343		
Psychosis	Mean		SD		
PANSS psychosis	12.964		5.548		
Depression					
CDS	2.107		2.781		
Cognition					
BACS	38.25		13.010		

medRxiv preprint doi: https://doi.org/10.1101/2024.07.11.24310281; this version posted December 7, 2024. The copyright holder for this preprint (which was not certified by peer review) is the author/funder, who has granted medRxiv a license to display the preprint in perpetuity. It is made available under a CC-BY 4.0 International license .

Psychosocial functioning		
PSP	4.964	1.895
Antipsychotic medication		
Dose in risperidone equivalent	6.152	4.331
Extrapyramidal syndrome		
SHRS	1.5	3.727
Number of hospitalizations in last 6 months*	0.045	0.213
Duration of illness (years)**	13.5	10.057

Abbreviations: SZ = schizophrenia; HC = healthy controls; SD = standard deviation; rs-fMRI = resting-state functional magnetic resonance imaging; BNSS = Brief Negative Symptom Scale; PANSS = Positive and Negative Syndrome Scale; CDS = Calgary Depression Scale for Schizophrenia; BACS = Brief Assessment of Cognition in Schizophrenia; PSP = Personal and Social Performance Scale; SHRS = St. Hans Rating Scale.

*Data not available for 2 patients.

**Data not available for 2 patients.

medRxiv preprint doi: https://doi.org/10.1101/2024.07.11.24310281; this version posted December 7, 2024. The copyright holder for this preprint (which was not certified by peer review) is the author/funder, who has granted medRxiv a license to display the preprint in perpetuity. It is made available under a CC-BY 4.0 International license .

medRxiv preprint doi: https://doi.org/10.1101/2024.07.11.24310281; this version posted December 7, 2024. The copyright holder for this preprint (which was not certified by peer review) is the author/funder, who has granted medRxiv a license to display the preprint in perpetuity. It is made available under a CC-BY 4.0 International license .

Investigation of cerebellar temporal coupling with the VTA in the validation cohort revealed seven spatially distinct cerebellum–VTA CAPs (Figure 4A; see Supplemental Materials for the selection of the optimal number of clusters). A prominent anti-coactivation pattern was again observed in the medial paravermal regions of Crus I and II. Pairwise spatial correlation analysis comparing the similarity of this anti-coactivation pattern with that from the main cohort at T1 confirmed spatial consistency (r = 0.93, $p < 0.001$; Figure 4B), suggesting a reproducible functional signature.

We examined the anti-coactivation pattern persistence and emergence between patients with schizophrenia and HC. We found no significant between-group differences in the metrics of this pattern. However, the anti-coactivation pattern emergence was significantly negatively correlated with the severity of apathy (*rho* = - 0.4, p= 0.022; Figure 4C, left panel), but not of diminished expression (*rho* = - 0.23, p= 0.128; Figure 4C, right panel), replicating our findings of the main cohort at T1. However, no associations with apathy were found for the pattern's persistence.

In a more granular examination, we found that the anti-coactivation pattern emergence in the validation dataset related to asociality (rho = -0.46, p= 0.012), replicating our findings from the main cohort. Of note, the relationship of the anti-coactivation pattern emergence with avolition was also close to significance (rho = -0.32, p= 0.066). We replicated these results using non-parametric permutations testing (apathy: *rho* = - 0.40, p = 0.043; asociality: *rho* = -0.46, p = 0.017) (see Figure S12 in the Supplemental Materials).

medRxiv preprint doi: https://doi.org/10.1101/2024.07.11.24310281; this version posted December 7, 2024. The copyright holder for this preprint (which was not certified by peer review) is the author/funder, who has granted medRxiv a license to display the preprint in perpetuity. It is made available under a CC-BY 4.0 International license .

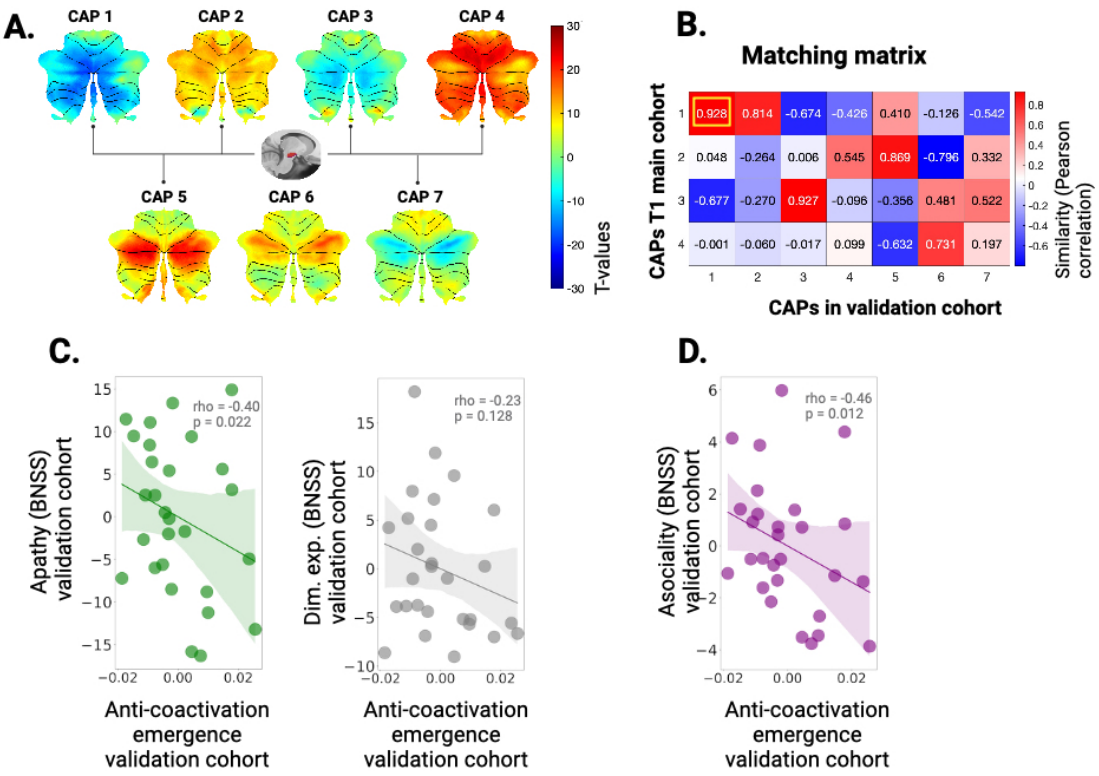

Figure 4. Validation cohort analysis: relation between anti-coactivation emergence and negative symptoms. A. Distinct spatial maps of cerebellar coactivation with the VTA in the validation cohort**.** B. Correlation matrix between coactivation patterns at T1 in the main cohort and coactivation patterns at T1 in the validation cohort. C. Reduced anti-coactivation emergence (CAP1 entry frequency) is associated with greater severity of apathy (in green). D. Reduced anti-coactivation emergence (CAP1 entry frequency) is associated with greater severity of asociality (in purple). *Note. Negative symptoms are quantified by the Brief Negative Symptom Scale (BNSS). Greater scores indicate more severe symptoms. Dim. exp. = diminished expression. The colorbar in panel A represents T-values, while that in panel B depicts similarity (Pearson correlation). Correlations are corrected for movement (mean framewise displacement) and antipsychotic medication (risperidone equivalent). Shaded areas on correlation plots C. and D. represent the 95% confidence interval*

medRxiv preprint doi: https://doi.org/10.1101/2024.07.11.24310281; this version posted December 7, 2024. The copyright holder for this preprint (which was not certified by peer review) is the author/funder, who has granted medRxiv a license to display the preprint in perpetuity. It is made available under a CC-BY 4.0 International license .

DISCUSSION

We uncovered a longitudinally stable spatial functional signature of anti-coactivation involving the cerebellar vermis and paravermis regions within Crus I – Crus II and the VTA in schizophrenia. This pattern was replicated into two distinct recordings (i.e., at baseline and at 3-month follow-up; Figure 2B) as well as in an independent sample with very high concordance (Figure 4B). Patients with scarcer emergence or reduced persistence of anti-coactivation had more severe apathy, suggesting that this pattern may be important for motivated behavior. Further, we observed a facetted relationship between features of the anti-coactivation and components of apathy: emergence appeared to more related to deficits of *wanting* – the drive to pursue a reward or goal, as indicated by its association with avolition and asociality, both reflecting reductions in goal-directed behavior or social motivational drive. In contrast, its persistence showed a stronger link to deficits of *liking* – the pleasure or positive emotional response derived from achieving or consuming a reward, specifically through anhedonia, reflecting diminished capacity for pleasure or positive emotional response. This distinction suggests that motivational and hedonic aspects may engage uniquely with anti-coactivation dynamics and evolve differently over time in ways that remains to be fully elucidated. Thus, anti-coactivation may serve as a biomarker for these distinct facets of apathy ultimately informing targeted interventions for specific components of apathy in schizophrenia that should be the focus of future research.

Our findings concord with evidence of a dysfunctional cerebellar ‘inhibitory tone’ over deeper structures (16,21) that could contribute to the excitatory/inhibitory (E/I)

medRxiv preprint doi: https://doi.org/10.1101/2024.07.11.24310281; this version posted December 7, 2024. The copyright holder for this preprint (which was not certified by peer review) is the author/funder, who has granted medRxiv a license to display the preprint in perpetuity. It is made available under a CC-BY 4.0 International license .

imbalance observed in schizophrenia (41). The balance between neuronal excitation and inhibition is crucial for optimizing the signal-to-noise ratio within neuronal networks (42). Dysregulation of cerebellar neurons projecting to the midbrain would disrupt the E/I and the signal-to-noise ratios, thereby diminishing the brain's ability to distinguish between rewarding and non-rewarding stimuli and thus leading to apathy (41). Given its anatomical structure with excitatory (*i.e.*, granule cells) and inhibitory neurons (*i.e.*, Purkinje cells), the cerebellum is a central hub for regulating both inhibition and excitation. The cerebellar Purkinje cells that coordinate the glutamatergic cerebellar output, have very high metabolic energy demands which makes them susceptible to damage (43) and thus prone to disturbing the E/I balance upon exposure to genetic and environmental stressors. Post-mortem studies of individuals with autism – a disorder also presenting with amotivated behavior and clinical overlap with schizophrenia – corroborated a reduced number of Purkinje cells, as well as alterations in cerebellar volume and connectivity (44). In sum, the cerebellum's critical role in gatekeeping cortical neuronal excitation and inhibition, coupled with its vulnerability to genetic and environmental stressors, points to its key role in the pathophysiology of amotivated behavior across schizophrenia and other developmental disorders.

In our study, we observed that features of the anti-coactivation pattern expressed in the *medial* (i.e., CAP1) but not the lateral cerebellum (i.e., CAP4) related to apathy over time (T2, T3). The implication of the medial cerebellum in the paravermis area provides further support for the Cognitive Dysmetria theory that postulated a key role of these regions in schizophrenia (45). The vermis and paravermis regions of Crus I and II, unlike their lateral counterparts, have unique molecular properties that may

medRxiv preprint doi: https://doi.org/10.1101/2024.07.11.24310281; this version posted December 7, 2024. The copyright holder for this preprint (which was not certified by peer review) is the author/funder, who has granted medRxiv a license to display the preprint in perpetuity. It is made available under a CC-BY 4.0 International license .

confer resilience to stress, enabling compensatory processes that require time in line with our findings (Figure 3). Specifically, Purkinje cells in these posterior cerebellar areas express zebrin-II, a highly conserved protein across vertebrates that provides resistance to injury (46), unlike the motor cerebellum, which is negative for zebrin-II and more susceptible to stress. This would imply that developmental stress impacts the motor cerebellum before non-motor areas. In this context, schizophrenia's clinical presentation could be viewed through cerebellar zebrin patterns, with initial "soft" neurological dysfunctions such as ataxia and dysmetria relying on motor areas (47) preceding negative and cognitive symptoms relying on the posterior cerebellum. Investigating the molecular mechanisms in these regions could enhance our understanding of dysfunctional cerebellar circuits in schizophrenia and should be the focus of future efforts (4,17).

Our study not only sheds light on the cerebellum regulatory role in the pathophysiology of apathy in schizophrenia, but also opens new avenues for therapeutic intervention. The specific cerebellar–VTA connectivity patterns that we identified offer promising targets for anti-coactivation -guided individualized cerebellar transcranial magnetic stimulation (TMS), aiming to restore functional neural circuits and alleviate negative symptoms in schizophrenia.

Our study has strengths and limitations. We identify for the first time and validate a longitudinally replicable anti-coactivation pattern of cerebellum–VTA connectivity in humans relating to negative symptoms in schizophrenia, bridging a critical gap on how the cerebellum regulates the reward circuitry over time. We employed an established method of dynamic functional connectivity (28,29,48–50), with strict

medRxiv preprint doi: https://doi.org/10.1101/2024.07.11.24310281; this version posted December 7, 2024. The copyright holder for this preprint (which was not certified by peer review) is the author/funder, who has granted medRxiv a license to display the preprint in perpetuity. It is made available under a CC-BY 4.0 International license .

quality control measures in place to ensure the reliability of our findings. We used a scale specifically designed to measure negative symptoms excluding items related to non-negative symptom psychopathology domains included in older scales (1,16) in line with the most recent guidelines (1). Following these guidelines, we utilized a clinical cohort with prominent negative symptoms and minimal confounding from psychosis, medication, or extrapyramidal effects. This approach enhances the validity of the mechanism-informed understanding of negative symptoms that we aimed to achieve in our work.

Regarding limitations, given that recruitment occurred during the COVID-19 pandemic, we encountered significant challenges for organizing and recruiting participants, leading to participant attrition between time points. Another limitation is the presence of predominantly male individuals, consistent with the literature and the gender repartition of schizophrenia in the population and, in particular, of negative symptoms in men (51). Future studies should examine sex differences in the expression of the patterns reported here. Finally, given our use of resting-state fMRI data, our measure of cerebellar activity is indirect. However, the blood oxygenation level-dependent signal has been linked to excitatory function (32), and therefore the observed anti-coactivation likely indicates either increased inhibition or reduced excitatory activity. To reflect this nuance, in this research we have employed the term "anti-coactivation" to remain agnostic about the exact underlying mechanism. However, future studies should aim to directly examine the specific neuronal activity and mechanisms underlying these patterns to provide a clearer understanding. In humans, this could be achieved through advanced imaging techniques like magnetoencephalography or invasive electrophysiological recordings in specific

medRxiv preprint doi: https://doi.org/10.1101/2024.07.11.24310281; this version posted December 7, 2024. The copyright holder for this preprint (which was not certified by peer review) is the author/funder, who has granted medRxiv a license to display the preprint in perpetuity. It is made available under a CC-BY 4.0 International license .

neurosurgical contexts, along with non-invasive neuromodulation techniques like TMS.

In conclusion, we identified that a longitudinally stable anti-coactivation pattern of the cerebellum with the VTA relates to apathy in schizophrenia. These results open new avenues for therapeutic interventions through resting-state anti-coactivation - targeted cerebellar neuromodulation for more effective and personalized treatments.

medRxiv preprint doi: https://doi.org/10.1101/2024.07.11.24310281; this version posted December 7, 2024. The copyright holder for this preprint (which was not certified by peer review) is the author/funder, who has granted medRxiv a license to display the preprint in perpetuity. It is made available under a CC-BY 4.0 International license .

Funding: Leenaards Foundation grant awarded to IB. PRD funds (22-2020-I) awarded to IB. Swiss National Science Foundation Grant No 169783 awarded to SK.

Contributions: Farnaz Delavari: Investigation, Methodology, Formal analysis, Writing original draft, Visualization. Jade Awada: Investigation, Formal analysis, Writing original draft, Visualization. Dimitri Van De Ville: Methodology, Review and editing of manuscript. Thomas A. Bolton: Methodology, Review and editing of manuscript. Mariia Kaliuzhna: Data acquisition. Fabien Carruzzo: Data acquisition. Noemie Kuenzi: Data acquisition. Teresa Marie Katthagen; Data Acquisition; Tal Geffen; Data Acquisition; Florian Schlagenhauf: Data acquisition. Fares Alouf: Data acquisition. Stephan Eliez: Review and editing of manuscript. Stefan Kaiser: Resources, Review and editing of manuscript. Indrit Bègue: Conceptualization, Investigation, Resources, Supervision, Project administration, Funding acquisition, Writing original manuscript.

Farnaz Delavari and Jade Awada contributed equally to this article.

Conflicts of interest: SK has received advisory board honoraria from Boehringer Ingelheim and Exeltis. The other authors report no conflicts of interests.

medRxiv preprint doi: https://doi.org/10.1101/2024.07.11.24310281; this version posted December 7, 2024. The copyright holder for this preprint (which was not certified by peer review) is the author/funder, who has granted medRxiv a license to display the preprint in perpetuity. It is made available under a CC-BY 4.0 International license .

REFERENCES

1. Galderisi S, Mucci A, Dollfus S, Nordentoft M, Falkai P, Kaiser S, et al. EPA guidance on assessment of negative symptoms in schizophrenia. Eur Psychiatry. 2021 Feb 8;64(1):e23, 1–23.
2. Kirkpatrick B, Fenton WS, Carpenter WT, Marder SR. The NIMH-MATRICS Consensus Statement on Negative Symptoms. Schizophr Bull. 2006 Apr;32(2):214–9.
3. Husain M, Roiser JP. Neuroscience of apathy and anhedonia: a transdiagnostic approach. Nat Rev Neurosci. 2018 Aug;19(8):470–84.
4. Bègue I, Kaiser S, Kirschner M. Pathophysiology of negative symptom dimensions of schizophrenia – Current developments and implications for treatment. Neurosci Biobehav Rev. 2020 Sep;116:74–88.
5. Manto M, Adamaszek M, Apps R, Carlson E, Guarque-Chabrera J, Heleven E, et al. Consensus Paper: Cerebellum and Reward. Cerebellum. 2024;
6. Van Overwalle F. Social and emotional learning in the cerebellum. Nat Rev Neurosci [Internet]. 2024 Oct 21 [cited 2024 Nov 10]; Available from: https://www.nature.com/articles/s41583-024-00871-5
7. Brady RO, Gonsalvez I, Lee I, Öngür D, Seidman LJ, Schmahmann JD, et al. Cerebellar-Prefrontal Network Connectivity and Negative Symptoms in Schizophrenia. Am J Psychiatry. 2019 Jul;176(7):512–20.
8. Laidi C, d'Albis MA, Wessa M, Linke J, Phillips M, Delavest M, et al. Cerebellar Volume in Schizophrenia and Bipolar I Disorder with and without Psychotic Features. Acta Psychiatr Scand. 2015 Mar;131(3):223–33.
9. Moberget T, Doan NT, Alnæs D, Kaufmann T, Córdova-Palomera A, Lagerberg TV, et al. Cerebellar volume and cerebellocerebral structural covariance in schizophrenia: a multisite mega-analysis of 983 patients and 1349 healthy controls. Mol Psychiatry. 2018 Jun 1;23(6):1512–20.
10. Cao H, Chén OY, Chung Y, Forsyth JK, McEwen SC, Gee DG, et al. Cerebello-thalamo-cortical hyperconnectivity as a state-independent functional neural signature for psychosis prediction and characterization. Nat Commun. 2018 Sep 21;9(1):3836.
11. Moberget T, Alnæs D, Kaufmann T, Doan NT, Córdova-Palomera A, Norbom LB, et al. Cerebellar Gray Matter Volume Is Associated With Cognitive Function and Psychopathology in Adolescence. Biol Psychiatry. 2019 Jul;86(1):65–75.
12. Andreasen NC, Paradiso S, O'Leary DS. 'Cognitive Dysmetria' as an Integrative Theory of Schizophrenia: A Dysfunction in Cortical-Subcortical-Cerebellar Circuitry? Schizophr Bull. 1998 Jan 1;24(2):203–18.
13. Tran KD, Smutzer GS, Doty RL, Arnold SE. Reduced Purkinje Cell Size in the Cerebellar Vermis of Elderly Patients With Schizophrenia. Am J Psychiatry. 1998 Sep;155(9):1288–90.
14. Nopoulos PC, Ceilley JW, Gailis EA, Andreasen NC. An MRI study of midbrain morphology in patients with schizophrenia: relationship to psychosis, neuroleptics, and cerebellar neural circuitry. Biol Psychiatry. 2001 Jan;49(1):13–9.
15. Daskalakis ZJ, Christensen BK, Fitzgerald PB, Fountain SI, Chen R. Reduced Cerebellar Inhibition in Schizophrenia: A Preliminary Study. Am J Psychiatry. 2005 Jun;162(6):1203–5.
16. Fernandez L, Major BP, Teo WP, Byrne LK, Enticott PG. Assessing cerebellar brain inhibition (CBI) via transcranial magnetic stimulation (TMS): A systematic

medRxiv preprint doi: https://doi.org/10.1101/2024.07.11.24310281; this version posted December 7, 2024. The copyright holder for this preprint (which was not certified by peer review) is the author/funder, who has granted medRxiv a license to display the preprint in perpetuity. It is made available under a CC-BY 4.0 International license .

review. Neurosci Biobehav Rev. 2018 Mar;86:176–206.
17. Bègue I, Brakowski J, Seifritz E, Dagher A, Tobler PN, Kirschner M, et al. Cerebellar and cortico-striatal-midbrain contributions to reward-cognition processes and apathy within the psychosis continuum. Schizophr Res. 2022 Aug;246:85–94.
18. Radua J, Schmidt A, Borgwardt S, Heinz A, Schlagenhauf F, McGuire P, et al. Ventral Striatal Activation During Reward Processing in Psychosis: A Neurofunctional Meta-Analysis. JAMA Psychiatry. 2015 Dec 1;72(12):1243–51.
19. Kostadinov D, Hausser M. Reward signals in the cerebellum: Origins, targets, and functional implications. Neuron. 2022;110(8):1290–303.
20. Carta I, Chen CH, Schott AL, Dorizan S, Khodakhah K. Cerebellar modulation of the reward circuitry and social behavior. Science. 2019 Jan 18;363(6424):eaav0581.
21. Baek SJ, Park JS, Kim J, Yamamoto Y, Tanaka-Yamamoto K. VTA-projecting cerebellar neurons mediate stress-dependent depression-like behaviors. eLife. 11:e72981.
22. Novello M, Bosman LWJ, De Zeeuw CI. A Systematic Review of Direct Outputs from the Cerebellum to the Brainstem and Diencephalon in Mammals. The Cerebellum. 2022 Dec 28;23(1):210–39.
23. Hoffman LJ, Foley JM, Leong JK, Sullivan-Toole H, Elliott BL, Olson IR. A Virtual In Vivo Dissection and Analysis of Socioaffective Symptoms Related to Cerebellum-Midbrain Reward Circuitry in Humans. J Neurosci Off J Soc Neurosci. 2024 Oct 9;44(41).
24. Snider RS, Maiti A. Cerebellar contributions to the papez circuit. J Neurosci Res. 1976 Jan 1;2(2):133–46.
25. Heath RG. Modulation of emotion with a brain pacemaker: Treatment for intractable psychiatric illness. J Nerv Ment Dis. 1977;165(5):300–17.
26. Hua JPY, Abram SV, Ford JM. Cerebellar stimulation in schizophrenia: A systematic review of the evidence and an overview of the methods. Front Psychiatry [Internet]. 2022 [cited 2024 Jul 10];13(1069488). Available from: https://www.frontiersin.org/articles/10.3389/fpsyt.2022.1069488/full
27. Basavaraju R, Ithal D, Thanki MV, Ramalingaiah AH, Thirthalli J, Reddy RP, et al. Intermittent theta burst stimulation of cerebellar vermis enhances fronto-cerebellar resting state functional connectivity in schizophrenia with predominant negative symptoms: A randomized controlled trial. Schizophr Res. 2021 Dec;238:108–20.
28. Liu X, Zhang N, Chang C, Duyn JH. Co-Activation Patterns in Resting-state fMRI Signals. NeuroImage. 2018 Oct 15;180(Pt B):485–94.
29. Liu X, Duyn JH. Time-varying functional network information extracted from brief instances of spontaneous brain activity. Proc Natl Acad Sci. 2013 Mar 12;110(11):4392–7.
30. Sheehan DV. The Mini-International Neuropsychiatric Interview (M.I.N.I.): The Development and Validation of a Structured Diagnostic Psychiatric Interview for DSM-IV and ICD-10. J Clin Psychiatry.
31. Kay SR, Fiszbein A, Opler LA. The Positive and Negative Syndrome Scale (PANSS) for Schizophrenia. Schizophr Bull. 1987 Jan 1;13(2):261–76.
32. Gerlach J, Korsgaard S, Clemmesen P, Lund Lauersen AM, Magelund G, Noring U, et al. The St. Hans Rating Scale for extrapyramidal syndromes: Reliability and validity. Acta Psychiatr Scand. 1993;87(4):244–52.
33. Chao-Gan Y, Yu-Feng Z. DPARSF: A MATLAB Toolbox for 'Pipeline' Data Analysis of Resting-State fMRI. Front Syst Neurosci. 2010;4:13.

medRxiv preprint doi: https://doi.org/10.1101/2024.07.11.24310281; this version posted December 7, 2024. The copyright holder for this preprint (which was not certified by peer review) is the author/funder, who has granted medRxiv a license to display the preprint in perpetuity. It is made available under a CC-BY 4.0 International license .

34. Bolton TAW, Wotruba D, Buechler R, Theodoridou A, Michels L, Kollias S, et al. Triple Network Model Dynamically Revisited: Lower Salience Network State Switching in Pre-psychosis. Front Physiol. 2020 Feb 11;11:66.
35. Kaiser RH, Kang MS, Lew Y, Van Der Feen J, Aguirre B, Clegg R, et al. Abnormal frontoinsular-default network dynamics in adolescent depression and rumination: a preliminary resting-state co-activation pattern analysis. Neuropsychopharmacology. 2019 Aug;44(9):1604–12.
36. Bolton TAW, Tuleasca C, Wotruba D, Rey G, Dhanis H, Gauthier B, et al. TbCAPs: A toolbox for co-activation pattern analysis. NeuroImage. 2020 May;211:116621.
37. Rolls ET, Huang CC, Lin CP, Feng J, Joliot M. Automated anatomical labelling atlas 3. NeuroImage. 2020 Feb;206:116189.
38. Delavari F, Sandini C, Kojovic N, Saccaro LF, Eliez S, Van De Ville D, et al. Thalamic contributions to psychosis susceptibility: Evidence from co-activation patterns accounting for intra-seed spatial variability (MCAPs). Hum Brain Mapp. 2024 Apr;45(5):e26649.
39. Gaviria J, Rey G, Bolton T, Ville DVD, Vuilleumier P. Dynamic functional brain networks underlying the temporal inertia of negative emotions. NeuroImage. 2021 Oct;240:118377.
40. Diedrichsen J, Zotow E. Surface-Based Display of Volume-Averaged Cerebellar Imaging Data. PLoS ONE. 2015 Jul 31;10(7):e0133402.
41. Andreasen NC, Pierson R. The Role of the Cerebellum in Schizophrenia. Biol Psychiatry. 2008 Jul;64(2):81–8.
42. Howes OD, Onwordi EC. The synaptic hypothesis of schizophrenia version III: a master mechanism. Mol Psychiatry. 2023 May;28(5):1843–56.
43. Kinnear Kern J. Purkinje cell vulnerability and autism: a possible etiological connection. Brain Dev. 2003 Sep;25(6):377–82.
44. Stoodley CJ, Tsai PT. Adaptive Prediction for Social Contexts: The Cerebellar Contribution to Typical and Atypical Social Behaviors. Annu Rev Neurosci. 2021 Jul 8;44:475–93.
45. Frazier MR, Hoffman LJ, Popal H, Sullivan-Toole H, Olino TM, Olson IR. A missing link in affect regulation: the cerebellum. Soc Cogn Affect Neurosci. 2022 Jun 22;17(12):1068–81.
46. Lin YC, Hsu CCH, Wang PN, Lin CP, Chang LH. The Relationship Between Zebrin Expression and Cerebellar Functions: Insights From Neuroimaging Studies. Front Neurol. 2020 Apr 22;11:315.
47. Samson GD, Lahti AC, Kraguljac NV. The neural substrates of neurological soft signs in schizophrenia: a systematic review. Schizophrenia. 2022 Apr 26;8(1):42.
48. Goodman ZT, Bainter SA, Kornfeld S, Chang C, Nomi JS, Uddin LQ. Whole-Brain Functional Dynamics Track Depressive Symptom Severity. Cereb Cortex. 2021 Oct 1;31(11):4867–76.
49. Yang H, Zhang H, Di X, Wang S, Meng C, Tian L, et al. Reproducible coactivation patterns of functional brain networks reveal the aberrant dynamic state transition in schizophrenia. NeuroImage. 2021 Aug;237:118193.
50. Huang Z, Zhang J, Wu J, Mashour GA, Hudetz AG. Temporal circuit of macroscale dynamic brain activity supports human consciousness. Sci Adv. 2020 Mar 13;6(11):eaaz0087.
51. Li X, Zhou W, Yi Z. A glimpse of gender differences in schizophrenia. Gen Psychiatry. 2022 Aug;35(4):e100823.

medRxiv preprint doi: https://doi.org/10.1101/2024.07.11.24310281; this version posted December 7, 2024. The copyright holder for this preprint
(which was not certified by peer review) is the author/funder, who has granted medRxiv a license to display the preprint in perpetuity.
It is made available under a CC-BY 4.0 International license .